Received: 2 October 2020 | Revised: 7 February 2021 | Accepted: 3 March 2021

DOI: 10.1111/jace.17802

Journal of the American Ceramic Society

ORIGINAL ARTICLE

Silver-doped sol-gel borate glasses: Dose-dependent effect on *Pseudomonas aeruginosa* biofilms and keratinocyte function

Shiva Naseri[1] | **Gabriele Griffanti**[1] | **William C. Lepry**[1] | **Vimal B. Maisuria**[2] | **Nathalie Tufenkji**[2] | **Showan N. Nazhat**[1]

[1]Department of Mining and Materials Engineering, McGill University, Montreal, QC, Canada

[2]Department of Chemical Engineering, McGill University, Montreal, QC, Canada

Correspondence
Showan N. Nazhat, Department of Mining and Materials Engineering, McGill University, Montreal, QC, Canada.
Email: showan.nazhat@mcgill.ca

Funding information
Fonds Québécois de la Recherche sur la Nature et les Technologies; Canada Foundation for Innovation; Natural Sciences and Engineering Research Council of Canada

Abstract

Borate-based glasses have generated great interest for wound healing applications due to their ability to incorporate biologically therapeutic ions which can then be released at the site of repair attributable to their high dissolution rates. In this study, the anti-bacterial activity and cytocompatibility of sol-gel–derived silver-doped borate glasses (AgBGs) of the compositional range $(60)B_2O_3$–$(36)CaO$–$(4–x)P_2O_5$–$(x)Ag_2O$, where x = 0.0, 0.3, 0.5, and 1 (mol.%) were investigated, *in vitro*. The dose-dependent anti-bacterial activity of AgBGs was demonstrated against *Pseudomonas aeruginosa* under both planktonic conditions and pre-formed biofilms, with up to 99.7% reduction in bacterial cell counts. Lower concentrations of ionic dissolution products from AgBGs were non-toxic to keratinocytes, stimulating their growth and metabolic activity. Furthermore, compositions containing 0.3 and 0.5 mol.% Ag significantly accelerated the migration of keratinocytes at two different concentrations in an *in vitro* 2D wound healing model. In summary, these therapeutic AgBGs have demonstrated potential for accelerated wound healing.

KEYWORDS

anti-inflammation, antimicrobial, bioactive glass, biofilm, borates, chronic wound, silver, sol-gel

1 | INTRODUCTION

The healing of full-thickness skin lesions is a significant clinical challenge especially for diabetic patients with chronic and infected wounds.[1] Current treatments using autografts, allografts, xenografts, and bioengineered skin tissue substitutes have many limitations, such as low bioactivity, the possibility of disease transmission, and limited availability.[2,3] For these reasons, wound dressings made from bioactive glasses are of growing interest as a promising solution for wound repair.[4-6] The majority of bioactive glasses are silicate based (*e.g.*, Bioglass® 45S5) and have been traditionally studied, and clinically applied, for mineralized tissue repair.[7-9] However, some silicate compositions such as "S53P4" also demonstrate anti-bacterial effectiveness against various bone infections[10-12] while others have shown anti-bacterial and wound healing potential.[4,13-17]

Borate-based bioactive glasses generally have higher dissolution rates compared to silicate-based glasses[18,19] and have received considerable interest for their wound repair properties.[6,20] In addition, their ability to release ions during dissolution has been implicated in healing mechanisms including anti-bacterial activity,[4,5] increasing cellular responses such as proliferation and migration, as well as stimulation of angiogenesis.[21] In both *in vitro* and *in vivo* studies, borate-based glasses have shown significantly higher wound closure and healing rates when compared to silicate-based glasses.[4,5] For example, in a full thickness skin defect model in rats, Zhou et al. showed that melt-quench borate glass micro-fibers of the composition (56.6)

B_2O–(5.5)Na_2O–(18.5)CaO–(11.1)K_2O–(4.6)MgO–(3.7)P_2O_5 (wt.%) had significantly higher blood vessel formation and wound closure rates than 45S5 glass microfibers, which was attributed to the presence of boron and its angiogenic ability.[21] In a similar model, Zhao et al. showed that melt-quench borate glass fibers of the composition (56.6)B_2O-(5.5)Na_2O-(18.5)CaO-(11.1)K_2O-(4.6)MgO-(3.7)P_2O_5 (wt.%) doped with CuO (0-3 wt.%) led to significantly higher rates of wound closure and blood vessel formation when compared to non-treated wounds.[22] More recently, it was reported that melt-quench borate bioactive glass microfibers had the capacity to heal skin defects in humans[23,24] along with a formulation (MIRRAGEN™, ETS Wound Care LLC) obtaining US Food and Drug Administration (FDA) clearance as a matrix for acute and chronic wound healing.[25]

Chronic wounds suffer from repeated tissue damage and infection, which prolongs the inflammation stage of the healing process.[1] Therefore, it is critical to reduce any infection risk during this phase as biofilms can form, inhibiting the healing process.[26] To this end, inorganic anti-bacterial therapeutics, such as copper, zinc, and silver, are of interest due to their low cost and potential for controlled release.[4] For example, copper- and zinc-doped borate glass fibers have recently been shown to be effective in reducing biofilm colonies of *Pseudomonas aeruginosa*, *Candida albicans*, *Staphylococcus aureus*, and *Acinetobacter baumannii*.[27] In addition to anti-bacterial activity,[28-30] silver (Ag^+) ions has also been demonstrated to have anti-inflammatory properties[31] as well as the ability to stimulate the migration of fibroblast cells to a wound site.[32] However, it is also known that higher dosages of the silver ions can be toxic to cells.[33] Depending on the biological environment and cell type, the toxic concentration of silver ions on mammalian cells has been reported to be in the range of 1 to 10 ppm.[33] Furthermore, given that silver-based biomaterials do not discriminate between pathogenic bacteria and healthy cells involved in wound healing,[34] it is imperative to evaluate both anti-bacterial activity and cytotoxicity to better understand the effects of silver ions on the healing process.

Recently, we have produced and fully characterized sol-gel–derived silver-doped borate glasses ["AgBGs"; (60)B_2O_3–(36)CaO–(4–X)P_2O_5–(X)Ag_2O, where X = 0.0, 0.3, 0.5 and 1 (mol.%)], which have demonstrated anti-bacterial efficacy against Gram-positive (*S. aureus*) and Gram-negative (*Escherichia coli*) bacteria, under both direct contact and ionic dissolution products.[35] Building on this, the objective of this *in vitro* study was to evaluate an optimum glass composition and concentration that demonstrates anti-bacterial activity while at the same time not impeding cellular functions. To this end, the anti-bacterial activity of these glasses was evaluated against *P. aeruginosa*, an opportunistic pathogen in chronic wounds with the ability to form resistant biofilms.[26]

Although less studied than fibroblasts, keratinocytes play a critical role in stimulating and coordinating the actions of multiple cell types involved in the healing process, such as the maintenance of tissue homeostasis and the recruitment of cells necessary for complete wound closure.[36] Keratinocyte migration is also imperative to wound healing since these cells are able to induce endothelial cell migration and angiogenesis in the wound site[37,38] as well as promote fibroblast proliferation and production of extracellular matrix.[39] It has previously been shown that gold nanoparticles[40] and silica-based bioactive glasses with gold[16,41] can stimulate the proliferation of keratinocytes. However, despite the importance of keratinocytes in wound healing, to our knowledge, these are the only bioactive glass studies that directly examined these cells. Furthermore, with regards to silver, much of the literature focuses on the effect of silver ions on the migration of fibroblastic cells to a wound area[32,42,43] and we are aware of only one other melt-quench silver-doped bioactive borate glass study.[44] Therefore, assessing the effect of our unique sol-gel–derived silver-doped bioactive borate glasses (AgBGs) on keratinocytes provides an opportunity to help better understand its potential in wound healing. In this study, we examine the direct effect of AgBG particles on bacteria as well as the dose effect of the ionic dissolution products of AgBGs on keratinocyte cell migration to assess their potential wound healing abilities.

2 | EXPERIMENTAL

2.1 | Sol-gel processing

Silver-doped, sodium-free borate-based glasses of the compositional range (60)B_2O_3–(36)CaO–(4–X)P_2O_5–(X)Ag_2O, where X = 0.0, 0.3, 0.5, and 1 (mol.%); B60, B60–0.3Ag, B60–0.5Ag, and B60–1Ag, respectively; were produced and characterized by the sol-gel process, as previously described.[35] Briefly, boric acid (≥99.5%; Sigma Aldrich) was initially mixed with anhydrous ethanol based on the solubility of boric acid (~11.2%) in a Teflon beaker, covered by a Teflon cap, and magnetically stirred at ~40°C for 30 min until the solution became clear. Triethyl phosphate (>99.8%; Sigma Aldrich) was then added and stirred for a further 30 min, followed by the addition of silver nitrate (Fisher Scientific) which was then stirred for another 30 min. Calcium methoxyethoxide (20% in methoxyethanol; Gelest) was then added and the sol was stirred for a final 30 min. The sol was transferred into polypropylene vials and aged for 5 days at 37°C. The aged sols were initially dried in a fume hood in air at room temperature (~21°C) for 2 days while covered with a non-transparent box to protect them from exposure to light followed by further drying at 120°C for 2 days. The dried as-made

powders were calcined at a rate of 3°C/min to 400°C with a 2 h dwell followed by furnace cooling. The glasses were ground and sieved to 25-75 μm particle size fraction using stainless steel wire mesh sieves and stored in a desiccator until analysis.

2.2 | Inductively coupled plasma optical emission spectrometry

Release of silver, boron, calcium, and phosphorus ions from glass powders in Dulbecco's modified Eagle's medium (DMEM; Sigma Aldrich), at a concentration of 1.5 mg/ml, was quantified using an inductively coupled plasma–optical emission spectrophotometer (ICP-OES, Thermo Scientific iCAP 6500). Aliquots of 2 ml were taken at 0.5, 6, and 24 h, filtered through a 0.2 μm nylon filter, and stored in a 15 ml falcon tube to which 4% (w/v) nitric acid (Fisher Scientific) was added followed by dilution with deionized water (DIW). Serially diluted solutions of boron (1, 10, 100 ppm), calcium (1, 10, 100 ppm), silver (0.05, 0.5, 5 ppm), and phosphorous (0.05, 0.5, 5 ppm) were used as standards.

2.3 | Anti-bacterial assessment

2.3.1 | Enumeration of colony forming units

The anti-bacterial activity of the AgBGs was examined using counts of colony forming units (CFU). An overnight grown culture of *P. aeruginosa* PA14 (UCBPP-PA14) was diluted in Mueller Hinton Broth II—cation adjusted (MHB-II, Oxoid; Fisher Scientific) to an $OD_{600\ nm}$ of 0.05. AgBGs at various concentrations (0.375, 0.75, 1.5, and 3 mg/ml) were mixed with diluted bacterial suspension in MHB-II. Bacterial cultures exposed to AgBGs for 24 h were serially diluted in phosphate-buffered saline (PBS) and plated on the surface of Luria-Bertani (LB) agar plates of 2 %w/v LB (Lennox, Fisher Scientific) powder and 1.5 %w/v agar powder (Fisher Scientific). The number of colonies was counted after 20 h of incubation at 37°C. All measurements were carried out in triplicate on different days.

2.3.2 | Bacteria growth curves

Bacterial growth was analyzed by directly exposing bacteria suspensions in MHB-II to AgBG particles (0.375 and 0.75 mg/ml) with an initial bacterial cell density of 0.05 $OD_{600\ nm}$. The optical density of the suspension was then measured (at 600 nm) for up to 72 h at 37°C using Tecan Infinite M200 Pro microplate reader (Tecan group Ltd.). All measurements were carried out in triplicate.

2.3.3 | Efficacy of AgBGs in biofilm eradication

A biofilm was formed by placing glass discs (1 cm diameter) into 24-well plates containing inoculum (0.05 $OD_{600\ nm}$) of *P. aeruginosa* PA14 in MHB-II and incubated overnight at 37°C. Then, the discs were washed gently using sterile PBS to remove non-adherent cells. After washing, discs were placed in a fresh 24-well plate containing 500 μL ionic dissolution products (filtered through a 0.2 μm nylon filter) of silver-doped borate glasses with silver content in the range of 0, 0.3, 0.5, and 1 mol.%; and glass concentration of 1.5 mg/ml in MHB-II and incubated at 37°C for 4 h. The discs were then removed and washed using PBS and placed in sterile tubes (Falcon) containing 2 ml of sterile PBS solution and sonicated in a bath sonicator (60 Hz and 150 W) for 10 min to disrupt any remaining biofilm. The culturable bacterial cell concentration in the resulting suspension was quantified using standard CFU counts as described above. All measurements were done in triplicate on different days.

2.4 | Assessment of keratinocyte function in the presence of AgBG dissolution products

2.4.1 | Cell culture

The HaCat human-derived keratinocyte cell line (kindly provided by Professor Anie Philip, McGill University) was cultured in T-75 culture flasks in DMEM supplemented with 10% fetal bovine serum (FBS; Hyclone) and 1% penicillin-streptomycin (an already mixed solution with 10 000 U/ml of penicillin and 10 000 μg/ml of streptomycin (Invitrogen)). Cells were incubated at 37°C under humidified air containing 5% CO_2. At 80% confluency, the cells were washed with sterile PBS, detached with 0.25% trypsin ethylenediaminetetraacetic acid solution (Wisent), and counted using a hemocytometer. Cells between passages 38 and 39 were used for cellular studies.

2.4.2 | Cell viability assay

HaCat cells were plated directly into 96-well assay plates at a density of 4000 cells/well and cultured in the presence of ionic release products generated from the dissolution of AgBGs at three concentrations in DMEM; 0.375, 0.75 (provided in supporting information), and 1.5 mg/ml (filtered through a 0.2 μm nylon filter). After 1, 4, and 7 days in

culture, cells were stained with 1 μM calcein-AM and 2 μM ethidium homodimer-1 (Live/Dead® assay; Invitrogen) for 15 min. Images of green fluorescent viable cells and red fluorescent dead cells were acquired in the same well plates using an Olympus IX81 inverted microscope equipped with a UPlanSApo 10 objective (UIS2 series). All conditions were tested in triplicate.

2.4.3 | Quantification of cell viability

HaCat cells were plated directly into 96-well assay plates at a density of 4000 cells/well and cultured in the presence of ionic release products generated from the dissolution of the AgBGs in DMEM at three concentrations; 0.375, 0.75, and 1.5 mg/ml. After 1, 4, and 7 days in culture, cells were incubated with 2 μM calcein-AM in 100 ml PBS. After 15 min, fluorescence was measured in the Mitras LB 940 microplate reader (Berthold Technologies, Germany) using a 485/535 nm excitation/emission filter pair. All conditions were tested in triplicate.

2.4.4 | Detection of cellular lactate dehydrogenase release

HaCat cells were plated directly into 24-well assay plates at a density of 50 000 cells/well and cultured in the presence of ionic release products generated from the dissolution of the AgBGs in DMEM at three concentrations; 0.375, 0.75, and 1.5 mg/ml. After 18, 24, and 48 hours, the cellular lactate dehydrogenase (LDH) release was evaluated (LDH Cytotoxicity Detection Kit; Clontech). LDH activity was measured from cells cultured in the presence of ionic release products generated from the dissolution of the AgBGs and compared to cells cultured in growth medium, in which the medium was used for background subtraction. Cell-free culture supernatant (100 μL aliquots) was collected in triplicate and then incubated up to 30 minutes with the reaction mixture according to manufacturer instructions. LDH activity was determined by measuring the absorbance of the samples at 490 nm using a microplate reader (Berthold Technologies, Germany) and then compared to the total LDH release by 50 000 cells/well killed in DMEM containing 1% Triton X-100 (Promega Corporation). Results are expressed relative to maximum LDH release.

2.4.5 | Assessment of cell metabolic activity

The AlamarBlue® assay (Invitrogen) was used to assess the effect of ionic dissolution products on the metabolic activities of HaCat cells. Cells were plated directly into 24-well assay plates at a density of 8 000 cells/well and cultured in the presence of ionic release products generated from the dissolution of the AgBGs in DMEM at three concentrations; 0.375, 0.75, and 1.5 mg/ml. At days 1, 4, and 7 in culture, the AlamarBlue® reagent (5%) was added to each well and, after 4 h incubation under darkness at 37°C in humidified air containing 5% CO_2, 100 ml aliquots were collected and transferred to a 96-well plate for analysis. The fluorescence intensity of reduced AlamarBlue® reagent was measured using a Mitras LB 940 microplate reader (Berthold Technologies) equipped with a 555 nm excitation filter and a 580 nm emission filter. After measurements have been completed, media in the 24-well plates were replaced for ongoing treatment. All conditions were tested in triplicate.

2.4.6 | Migration assay

The effect of the AgBG ionic dissolution products on the migration of HaCat cells was assessed using the ibidi™ Culture-Insert 3 Well. Cells at a density of 270 000 cells/well were initially cultured in each well for 24 h in DMEM in a humidified incubator at 37°C and under 5% CO_2. After 24 h, the Culture-Insert was gently removed using sterile tweezers followed by washing the cells with PBS twice. The uniform scratch was observed. Then, the culture medium was supplemented with ionic release products generated from the dissolution of the AgBGs in DMEM at two concentrations (0.75 and 1.5 mg/ml) and cultured for a further 24 h. Cells cultured with neat DMEM were used as control. Cell migration was observed with an inverted microscope (Leica DMI 3000B), and images were taken with a CCD camera (Leica DFC 420C). The original and final area of a scratch after 24 h were measured to calculate the scratch shrinkage percentage ($n = 4$).

2.5 | Statistical analysis

Data for each assay time point were analyzed for statistical significance between conditions using the Student t-test at a significance level of $p < .05$.

3 | RESULTS AND DISCUSSION

3.1 | Glass dissolution and ion release in culture medium

ICP-OES analysis was carried out to examine the ionic release profiles from the dissolution of AgBG particles (Figure S1; scanning electron microscopy images of the glass particles) after immersion in cell culture medium (Figure 1).

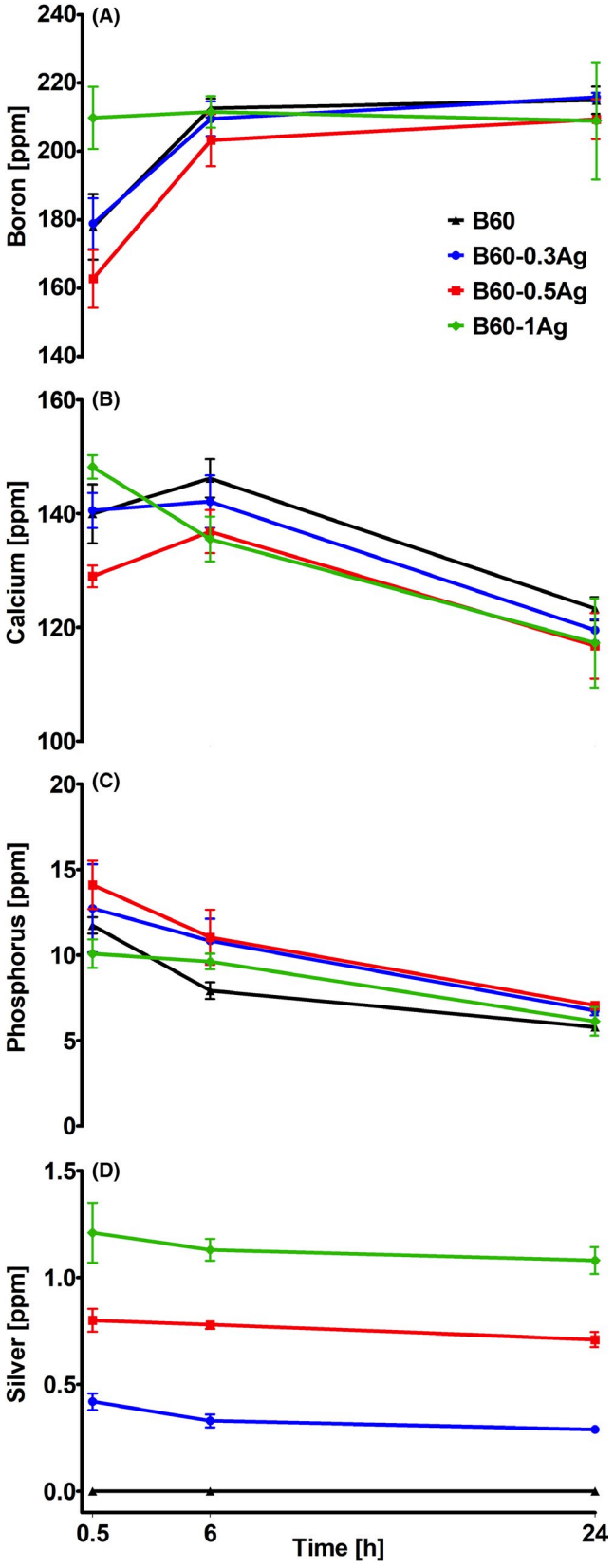

FIGURE 1 AgBG ionic dissolution products of (A) boron, (B) calcium, (C) phosphorus, and (D) silver in cell culture medium, as measured using ICP-OES (error bars =standard deviation (SD), $n = 3$)

The total boron and calcium ion release in cell culture medium were in agreement with their equivalents in deionized water.[35] Furthermore, phosphorus and calcium ion release decreased over time, which may be due to the formation of calcium-phosphate precipitates.[45] The ionic release patterns is typical of our previously made highly reactive sol-gel–derived bioactive borate glasses and suggests rapid dissolution rates within 0.5 h.[35,46-50] The extent of silver ions release from the glasses increased with its doping levels in the AgBGs. However, silver ions release in cell culture medium was lower than that observed in DIW,[35] which can be attributed to the presence of chloride ions as well as organic compounds in the culture medium, potentially forming silver complexes.[51]

3.2 | Determination of anti-bacterial efficacy of AgBG against P. aeruginosa PA14

Anti-bacterial efficacy of AgBGs at different concentrations was investigated against the wound-associated pathogen, *P. aeruginosa* PA14, in both planktonic and biofilm growth modes. *P. aeruginosa* is an opportunistic Gram-negative pathogen causing both acute and chronic infections,[52] and is difficult to eradicate in skin-related infections since it has an intrinsic antibiotic resistance, resulting in the formation of chronic wounds.[26] The CFU assay showed that the ionic dissolution products of AgBGs were effective against *P. aeruginosa* PA14 in a dose-dependent manner (Figure 2A). For example, AgBGs with 0.5 or 1 mol.% silver were 100% effective in killing the bacteria even at the lower concentration of 0.375 mg/ml, while B60–0.3Ag was only effective at the concentration of 1.5 mg/ml. Additionally, the non-silver–doped glasses (B60) demonstrated some anti-bacterial activity at the concentration of 3 mg/ml, where the culturable cell counts exhibited a slight decrease. This may be attributed to the increase in local pH[53,54] as a consequence of glass dissolution products.[4,9] For example, in the case of the B60 composition, our previous work has reported that after 24 h immersion in DIW, B60 dissolution resulted in a pH increase to up to ~9.[35] Furthermore, it has been reported that an increase in ionic release products also potentially results in an increase in osmotic pressure, which influences the viability of bacteria.[53,54]

To further evaluate the dose-dependent anti-bacterial activity of the AgBGs, the growth of *P. aeruginosa* PA14 planktonic cells was measured when directly exposed to the glass particles. Figure 2B,C show the growth curves of PA14 when exposed to 0.375 and 0.75 mg/ml of AgBGs up to 72 h, respectively. It was demonstrated that B60-1Ag glass particles inhibited the growth of PA14 up to 72 h at both glass

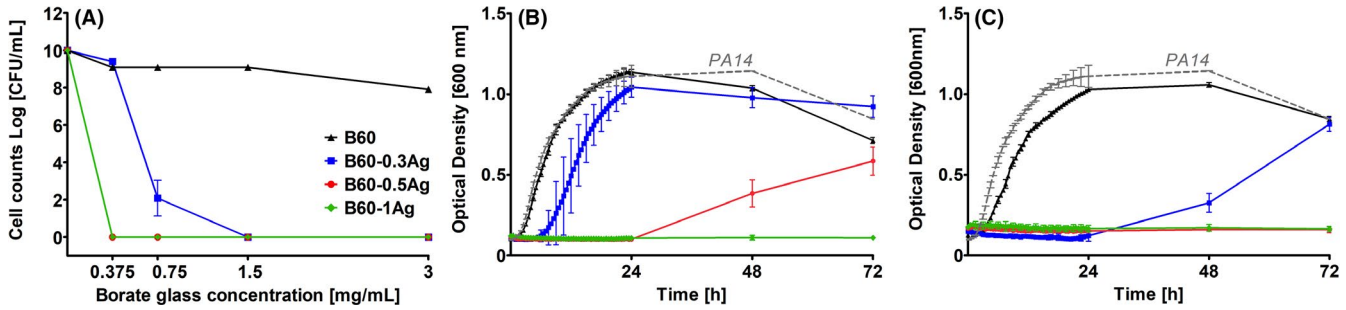

FIGURE 2 Anti-bacterial efficacy of the AgBG compositional range. (A) Culturable cell count of *P. aeruginosa* PA14 after exposure to AgBG particles of different silver content and glass concentration. Growth curves of *P. aeruginosa* PA14 (PA14-only control represented by gray curve) at glass concentrations of (B) 0.375 and (C) 0.75 mg/ml (without and with silver content), respectively. (Error bars: SD, $n = 3$)

concentrations, while B60–0.5Ag glass particles were able to inhibit bacterial growth up to 24 h even at a concentration of 0.375 mg/ml. In the case of B60–0.3Ag, the higher concentration of 0.75 mg/ml was required to inhibit bacterial growth and only up to 24 h. Non-silver–doped glasses (B60), on the other hand, did not inhibit bacterial growth.

In order to test the activity of AgBGs against biofilms, the effect of ionic dissolution products from AgBGs at a concentration of 1.5 mg/ml on pre-formed *P. aeruginosa* PA14 biofilms was investigated (Figure 3). The results were compared to a control (untreated PA14 biofilms), where the biofilms were treated only with MHB-II (white color bar). The culturable cell counts decreased with increasing silver content from 0.3 to 1 mol.% in the glass formulation in comparison with the control biofilm (Figure 3A). A 99.7% reduction in CFU count was achieved when the biofilm was treated with ionic dissolution products from B60–1Ag (Figure 3B). These results confirm the correlation between silver content in the AgBG composition and anti-bacterial activity in a dose-dependent manner. Overall, the anti-bacterial analysis suggests that silver-doped glasses inhibit the growth and biofilms of *P. aeruginosa* PA14 over a prolonged incubation period.

3.3 | Effect of AgBG ionic dissolution products on keratinocyte viability and metabolic activity

In order to evaluate the effect of silver ions on keratinocytes, the Live/Dead assay was carried out on HaCat cells treated with AgBG ionic dissolution products at concentrations of 0.375, 0.75, and 1.5 mg/ml and visualized up to 7 days in culture (Figures 4, S2, and S3, respectively). In general, under all conditions, there was an increasing trend in the density of viable cells from days 1 to 7. At day 1, predominantly live cells were observed independent of silver content. By day 4, the silver-treated cultures revealed a higher density of viable cells despite the presence of some dead cells. However,

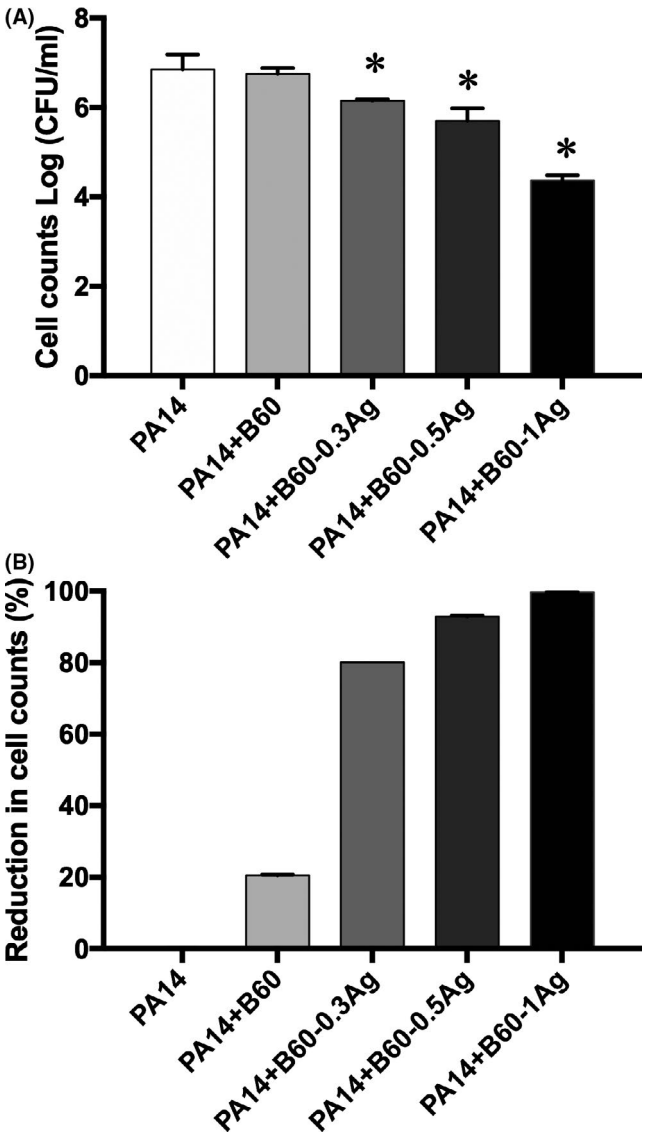

FIGURE 3 The effect of ionic dissolution products of AgBGs with glass concentration of 1.5 mg/ml on (A) CFU counts, and (B) equivalent reduction in CFU counts of PA14 biofilm, when compared to control biofilm (error bars: SD, $n = 3$), Statistically significant (*) compared to the control biofilm (PA14) ($p < .05$)

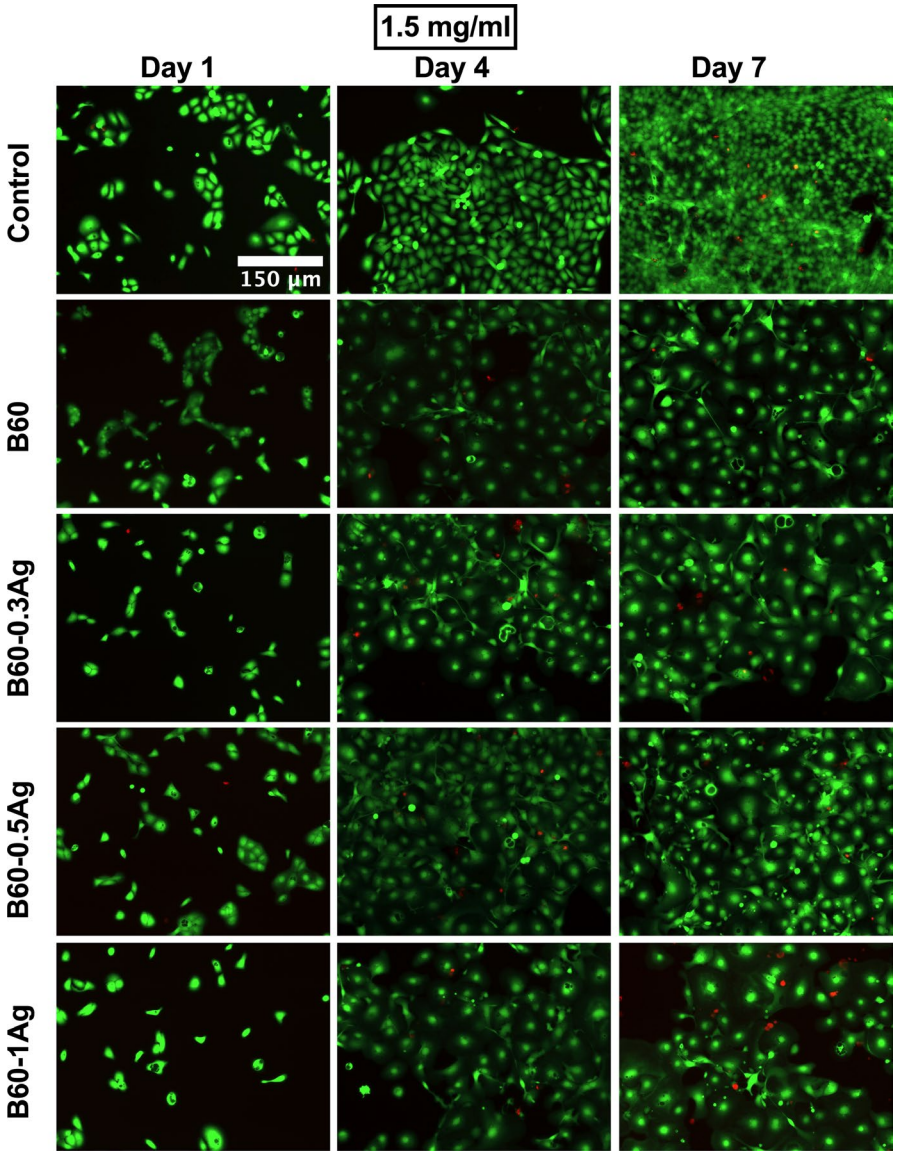

FIGURE 4 Calcein-AM stained live HaCat cells (green) and ethidium homodimer-1 stained dead cells (red) at days 1, 4, and 7 in culture supplemented with ionic dissolution products of AgBGs at concentration of 1.5 mg/ml, scale bar =150 µm

at day 7 the presence of viable cells was lower in B60–1Ag when compared to the other conditions. In general, presence of silver ions at lower concentrations did not indicate toxicity against keratinocytes since only a low number of dead cells was observed. The results also indicate that the proliferation rate of cells was qualitatively slower in the presence of silver ions than those in the control medium.

To better evaluate the effect of ionic release products on HaCat cell viability, the fluorescence of Calcein-AM stained live cells was measured (Figure 5A). In general, there was an increasing trend in the viability of cells from days 1 to 7, independent of conditioning, except for the B60–1Ag when applied at the higher concentrations of 0.75 and 1.5 mg/ml. The non-silver–doped glasses (B60) were compared with the control medium at all three concentrations to evaluate the effect of boron on cell viability. At 0.375 and 0.75 mg/ml concentrations, there was no significant difference between B60 and the control group, indicating that boron did not affect cell viability at lower concentrations (Figure 5A(i and ii)). However, in line with the Live/Dead assay, the higher concentration of B60 (*i.e.*, 1.5 mg/ml) showed a significant reduction in cell viability, when compared to those cultured in the control medium (Figure 5A(iii)).

To better understand the effect of silver ions on HaCat cell viability, the effect of the ionic dissolution products from the silver-doped glasses was compared to that of the baseline formulation (B60). At a concentration of 0.375 mg/ml, cell viability was increased with an increase of up to 0.5 mol.% silver. However, a further increase in the silver content up to 1 mol.% caused a decrease in keratinocyte cell viability at days 4 and 7 (Figure 5A). At a concentration of 0.75 mg/ml, it was observed that cell viability in the presence of B60-1Ag was significantly reduced at day 7 when compared to the B60 treatment (Figure 5A(i)). Figure 5A(iii) shows the viability of HaCat cells when exposed to the glass ionic dissolution products in cell culture medium at a concentration

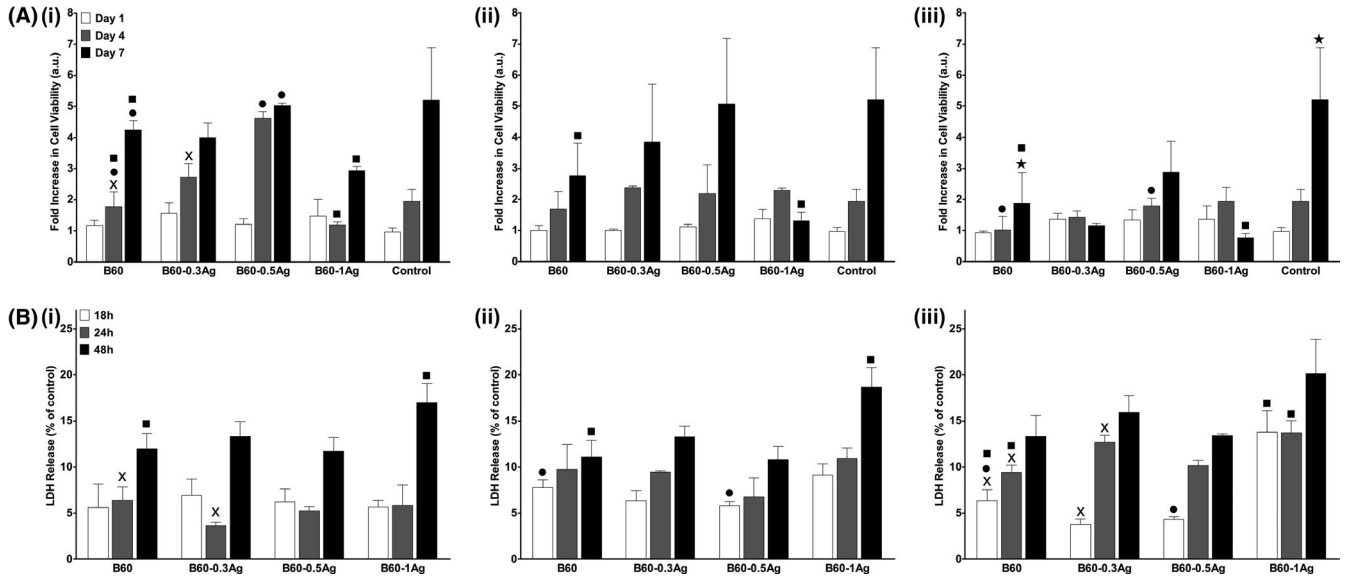

FIGURE 5 (A) HaCat cell viability (expressed as fold increase relative to control at day 1) determined from the fluorescence signal of calcein-AM stained live cells, treated with ionic dissolution products of AgBGs at concentrations of (i) 0.375, (ii) 0.75, and (iii) 1.5 mg/ml for up to 7 days in culture (error bars: SD, $n = 3$). (B) Cellular release of LDH after exposure to ionic dissolution products of AgBGs at concentrations of (i) 0.375, (ii) 0.75, and (iii) 1.5 mg/ml for up to 48 hours. Significance ($p < .05$) is represented as ★for B60 vs. control, x for B60-0.3Ag vs. B60, ● for B60-0.5Ag vs. B60, and ■ for B60-1Ag vs. B60

of 1.5 mg/ml. At day 4, there was an increase in cell viability with an increase in silver content up to 0.5 mol.%, which then decreased with a further increase in silver content up to 1 mol.%. Furthermore, it can be inferred that an optimum silver ion concentration (less than 1 ppm; B60-0.3Ag and B60-0.5Ag formulations) in the cell culture medium enhanced keratinocyte viability. Deviation from this concentration may result in an adverse effect on HaCat cell viability. Furthermore, the cellular release of LDH was evaluated in order to investigate the effect of silver ions on cell mortality (Figure 5B). Cell mortality trends were similar in all samples. However, cytotoxicity effects were observed at 48 hours from all AgBG concentrations when cells were exposed to ionic dissolution products from B60-1Ag, which is in agreement with previous findings.[44]

Figure 6 shows the metabolic activity of HaCat cells cultured over 7 days in media conditioned with ionic dissolution products from AgBGs at concentrations of 0.375, 0.75, and 1.5 mg/ml. In general, there was an increasing trend in the proliferation rates of keratinocyte cells from days 1 to 7, independent of the condition. The non-silver–doped glasses (B60) were compared with the control medium at all three concentrations to evaluate the effect of boron on metabolic activity. At the concentrations of 0.375 and 0.75 mg/ml, the ionic dissolution products from B60 showed no significant difference in metabolic activity when compared to the control. However, at a higher concentration of 1.5 mg/ml, there was lower metabolic activity in comparison with the control medium at days 4 and 7. The effect of the ionic dissolution products from the silver-doped glasses was compared to that of the baseline formulation (B60) to better understand the effect of silver on HaCat metabolic activity. At concentrations of 0.375 and 0.75 mg/ml, silver content in the culture medium did not affect the metabolic activity. However, at day 7 in culture, exposure to ionic dissolution products from B60-0.3Ag at the higher concentration of 1.5 mg/ml caused an increase in the metabolic activity of the HaCat cells relative to those cultured in the presence of the B60 ionic products.

AlamarBlue® reduction also indicated that the higher concentration of 1.5 mg/ml of non-silver–doped glasses led to a lower metabolic activity when compared with the control at days 4 and 7. This reduction in metabolic activity may be due to a high concentration of boron and its potential toxic effect on the HaCat cells, inhibiting both their proliferation and metabolic activity.[55] This finding suggests that silver ions suppressed and compensated the adverse effect of boron on cell metabolism. To further assess the potential of AgBGs in wound healing, the dose effect of their ionic dissolution products on the viability and metabolic activity of NIH/3 T3 fibroblast cells was investigated (Figures S4 and S5).

Taken together, these results suggest that under static conditions, higher concentrations of boron may be toxic to cells, which is in agreement with previous reports.[55] It has also been suggested that the toxic effects of boron can be reduced or eliminated under dynamic flow conditions, which better simulate in vivo environments.[21,22] For example, Brown et al., investigated the *in vitro* biological response of biomaterials for wound healing applications and showed that there is a need for a more reliable method to better mimic in vivo conditions.[56] It was proposed that *in vitro* culturing

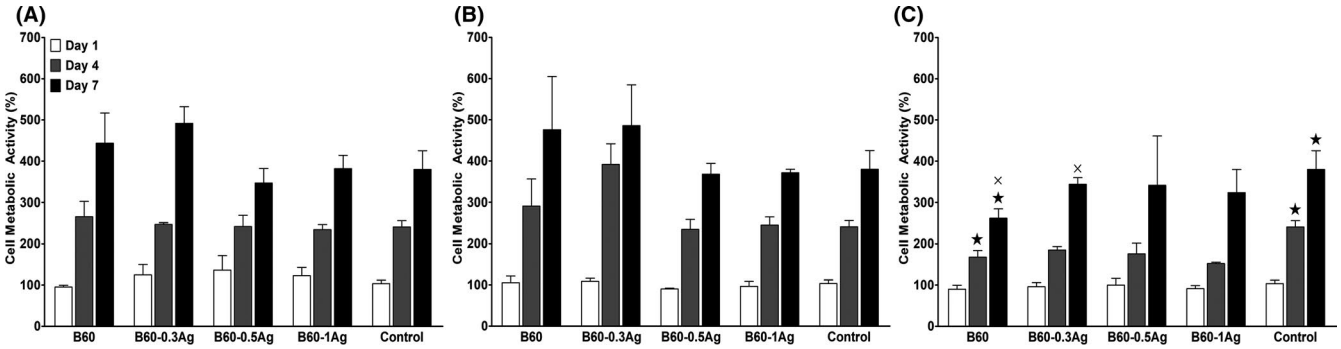

FIGURE 6 Metabolic activity (expressed as percentage relative to control at day 1) of HaCat cells treated with ionic dissolution products of AgBGs at concentrations of (A) 0.375, (B) 0.75, and (C) 1.5 mg/ml for up to 7 days in culture (error bars: SD, $n = 3$). Significance ($p < .05$) is represented as ★for B60 vs. control and x for B60-0.3Ag vs. B60

under moderate dynamic conditions may result in a higher cell density and lower toxicity when compared with static conditions.[56] Furthermore, Yang et al., demonstrated that the viability and proliferation rate of human skin fibroblast cells can be improved under optimized dynamic flow rates.[55] It was mentioned that under static conditions, which is in contrast to the natural wound healing environment, the local increase in boron concentration can be highly toxic to cells.[55] While these dynamic flow conditions might ease the toxic effects of boron, it may also reduce the effectiveness of silver. Nevertheless, it is important to note that in a clinical setting, there are typically multiple applications of the glass, which would also result in a more sustained anti-bacterial effect.

The results in this study also indicate that the addition of silver into the glass network can enhance cell viability in comparison with the non-silver–doped formulation. For example, glasses containing 0.5 mol.% (1.7 wt.%) silver were not toxic to keratinocytes and fibroblastic cells. This is in agreement with previous works on the effect of Ag particles on keratinocytes.[57,58] In particular, while higher concentrations of Ag^+ ions ($>10^{-4}$ mol/L) are known to be cytotoxic to HaCat cells,[59,60] lower concentrations (10^{-6} and 10^{-5} mol/L) promote their proliferation.[61] This may be due to the alteration of the cellular redox state, which results in the generation of reactive oxygen species (ROS), likely leading to its cytotoxic effect. On the other hand, low concentrations of ROS are also important in the intracellular signal transduction pathway involved in cell proliferation. As previously reported, Ag^+ ions play a role in generating ROS in HaCat cells[61] and at low concentrations, silver may induce a moderate increase in ROS levels, ultimately enhancing mitochondrial metabolism and promoting DNA replication. Furthermore, Ag particles have been shown to enhance the expression of keratinocyte growth factor 2, a protein that stimulates the proliferation and migration of HaCat cells.[62]

This study has also underscored the importance of investigating both the anti-bacterial activity and potential cytotoxic effects of silver-based biomaterials for wound healing applications. It has previously been shown that both keratinocytes and fibroblasts are susceptible to damage when exposed to high concentrations of silver, despite of its beneficial effect in reducing inflammation and accelerating the early phases of wound healing.[34] Studies on bioactive borate glass with up to 1 wt.% silver have demonstrated anti-bacterial activity against *S. epidermidis* and *methicillin*-resistant *S. aureus* (MRSA),[63] as well as *Escherichia Coli*.[64] On the other hand, distinct studies have shown that the ionic dissolution products from borate glasses with 0.75 and 1 wt.% Ag_2O were not toxic to osteoblastic and fibroblastic cells, whereas glasses with 2 wt.% Ag_2O were toxic.[44]

3.4 | Effect of AgBG ionic dissolution products on the migration of keratinocytes

Since the ionic dissolution products from glasses dissolved in medium at 0.75 and 1.5 mg/ml demonstrated higher anti-bacterial efficacy, these concentrations were used to investigate the effect of AgBGs on HaCat cell migration (Figure 7). Keratinocyte migration has been implicated in inducing endothelial cell migration and angiogenesis as well as promoting fibroblast proliferation and extracellular matrix production, thus aiding the healing process.[37-39] At 0 h (Figure 7A), scratches of similar width (500 ± 50 μm) were made on the base of each well cultured with HaCat cells using the Culture-Insert™ and, after 24 h in culture, the scratches in the control and non-doped glass (B60) treatment were slightly reduced. However, the width of the scratch in the silver-doped glasses at the concentrations of 0.75 and 1.5 mg/ml indicated a greater decrease after 24 h (Figure 7B). Measurement of the remaining scratch area of the 0.3 and 0.5Ag compositions at 24 h (Figure 7C) showed a significant scratch reduction at both concentrations, when compared to the control. In particular, B60-0.5Ag demonstrated almost full scratch reduction, indicating that the AgBG ionic dissolution products stimulated HaCat cell migration. Furthermore, both B60-0.3Ag at

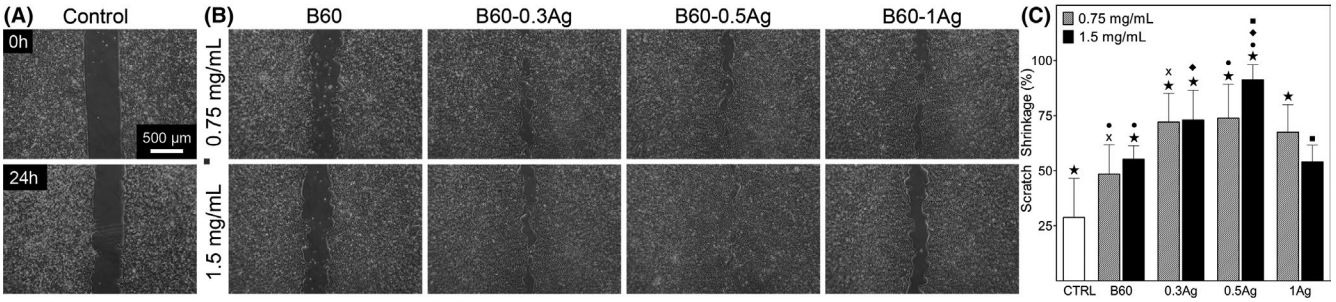

FIGURE 7 Representative images of (A) HaCat cells at 0 and 24 h cultured with control medium and (B) the migration of the cells due to the ionic dissolution products of AgBGs at concentrations of 0.75 and 1.5 mg/ml after 24 h. (C) Statistical analysis of scratch distance shrinkage of glass concentration of 0.75 and 1.5 mg/ml after 24 h. The original and final area of a scratch were measured to calculate the scratch shrinkage percentage (error bars: SD, $n = 4$). Significance ($p < .05$) represented as ★for each condition vs. control, x for B60–0.3Ag vs. B60, ● for B60-0.5Ag vs. B60, ◆ for B60–0.3Ag vs. B60–1Ag at 1.5 mg/ml, and ■ for B60–0.5Ag vs. B60-1Ag at 1.5 mg/ml

1.5 mg/ml and B60-1Ag at 0.75 mg/ml showed significant reduction compared to the control. Moreover, both concentrations of B60-0.5Ag significantly reduced the scratch area compared to B60, whereas at 0.75 mg/ml, only B60-0.3Ag showed a significant ($P < .05$) difference compared to B60. On the other hand, for 1.5 mg/ml concentrations, both the 0.3 and 0.5Ag compositions significantly reduced the scratch area compared to B60-1Ag which suggests a maximum limit for silver doping, as has been previously observed in other studies.[44] Taken together, these results suggest that at a concentration of less than 1 ppm silver ion has the ability to stimulate keratinocyte cell migration, which may be replicated in a wound site to potentially accelerate the healing process, while at higher concentrations may cause adverse effects.

4 | CONCLUSIONS

Therapeutic, silver-doped sol-gel–derived borate glasses have demonstrated promise in accelerating wound healing. AgBGs inhibited the growth of *P. aeruginosa* PA14 up to 3 days and eradicated biofilm cells by up to 99.7%. It was also demonstrated that AgBG ionic dissolution products, mainly silver, were not toxic to HaCat and NIH/3 T3 cells at low concentrations. However, the high boron content of the glasses may be a source of toxicity, underscoring the importance of investigating both anti-bacterial activity and potential cytotoxic effects. Moreover, a 2D *in vitro* model demonstrated that compositions doped with 0.3 and 0.5 mol.% Ag, at two concentrations, promoted keratinocyte migration and significantly decreased the wound area. Therefore, both silver doping and glass concentration may be altered to optimize anti-bacterial activity and cellular responses for target applications. Future work will investigate the effect of these glasses on the wound healing process under dynamic conditions, *in vitro* as well as through in vivo models.

ACKNOWLEDGMENTS

This study was supported by the Natural Sciences and Engineering Research Council of Canada, Canada Foundation for Innovation, Aligo Innovation, McGill University Faculty of Engineering Innovations Fellowship, and McGill Engineering Doctoral Award. N.T. also acknowledges the Canada Research Chairs program. The authors would like to thank Professor Anie Philip and Dr. Kenneth Finnson (McGill University) for providing HaCat cells and Dr. Mira Okshevsky for assistance in taking the microscope images.

ORCID

William C. Lepry https://orcid.org/0000-0002-3980-209X
Nathalie Tufenkji https://orcid.org/0000-0002-1546-3441
Showan N. Nazhat https://orcid.org/0000-0002-8134-183X

REFERENCES

1. Stadelmann WK, Digenis AG, Tobin GR. Physiology and healing dynamics of chronic cutaneous wounds. Am J Surg. 1998;176(2a):26s–38s.
2. Ma L, Gao C, Mao Z, Zhou J, Shen J, Hu X, et al. Collagen/chitosan porous scaffolds with improved biostability for skin tissue engineering. Biomaterials. 2003;24(26):4833–41.
3. Metcalfe AD, Ferguson MWJ. Bioengineering skin using mechanisms of regeneration and repair. Biomaterials. 2007;28(34):5100–13.
4. Naseri S, Lepry WC, Nazhat SN. Bioactive glasses in wound healing: hope or hype? J Mater Chem B. 2017;5(31):6167–74.
5. Rahaman MN, Day DE, Sonny Bal B, Fu Q, Jung SB, Bonewald LF, et al. Bioactive glass in tissue engineering. Acta Biomater. 2011;7(6):2355–73.
6. Miguez-Pacheco V, Hench LL, Boccaccini AR. Bioactive glasses beyond bone and teeth: emerging applications in contact with soft tissues. Acta Biomater. 2015;13:1–15.
7. Xynos ID, Edgar AJ, Buttery LDK, Hench LL, Polak JM. Ionic products of bioactive glass dissolution increase proliferation of human osteoblasts and induce insulin-like growth factor II mRNA expression and protein synthesis. Biochem Biophys Res Commun. 2000;276(2):461–5.

8. Jones JR, Brauer DS, Hupa L, Greenspan DC. Bioglass and bioactive glasses and their impact on healthcare. Int J Appl Glass Sci. 2016;7(4):423–34.
9. Jones JR. Review of bioactive glass–from Hench to hybrids. Acta Biomater. 2013;9(1):4457–86.
10. Coraça-Huber DC, Fille M, Hausdorfer J, Putzer D, Nogler M. Efficacy of antibacterial bioactive glass S53P4 against S. aureus biofilms grown on titanium discs *in vitro*. J Orthop Res. 2014;32(1):175–7.
11. Lindfors NC, Hyvönen P, Nyyssönen M, Kirjavainen M, Kankare J, Gullichsen E, et al. Bioactive glass S53P4 as bone graft substitute in treatment of osteomyelitis. Bone. 2010;47(2):212–8.
12. van Gestel NAP, Geurts J, Hulsen DJW, van Rietbergen B, Hofmann S, Arts JJ. Clinical applications of S53P4 bioactive glass in bone healing and osteomyelitic treatment: a literature review. BioMed Res Int. 2015;2015:684826.
13. Popa AC, Fernandes HR, Necsulescu M, Luculescu C, Cioangher M, Dumitru V, et al. Antibacterial efficiency of alkali-free bioglasses incorporating ZnO and/or SrO as therapeutic agents. Ceram Int. 2019;45(4):4368–80.
14. Fernandes HR, Gaddam A, Rebelo A, Brazete D, Stan GE, Ferreira JMF. Bioactive glasses and glass-ceramics for healthcare applications in bone regeneration and tissue engineering. Materials. 2018;11(12):2530.
15. Chen S, Huan Z, Zhang L, Chang J. The clinical application of a silicate-based wound dressing (DermFactor®) for wound healing after anal surgery: a randomized study. Int J Surg. 2018;52:229–32.
16. Mârza SM, Magyari K, Bogdan S, Moldovan M, Peştean C, Nagy A, et al. Skin wound regeneration with bioactive glass-gold nanoparticles ointment. Biomed Mater. 2019;14(2):025011.
17. Norris E, Ramos-Rivera C, Poologasundarampillai G, Clark JP, Ju Q, Obata A, et al. Electrospinning 3D bioactive glasses for wound healing. Biomed Mater. 2020;15(1):015014.
18. Yao A, Wang D, Huang W, Fu Q, Rahaman MN, Day DE. In vitro bioactive characteristics of borate-based glasses with controllable degradation behavior. J Am Ceram Soc. 2007;90(1):303–6.
19. Huang W, Day DE, Kittiratanapiboon K, Rahaman MN. Kinetics and mechanisms of the conversion of silicate (45S5), borate, and borosilicate glasses to hydroxyapatite in dilute phosphate solutions. J Mater Sci Mater Med. 2006;17(7):583–96.
20. Balasubramanian P, Büttner T, Miguez Pacheco V, Boccaccini AR. Boron-containing bioactive glasses in bone and soft tissue engineering. J Eur Ceram Soc. 2018;38(3):855–69.
21. Zhou J, Wang H, Zhao S, Zhou N, Li L, Huang W, et al. In vivo and *in vitro* studies of borate based glass micro-fibers for dermal repairing. Mater Sci Eng C Mater Biol Appl. 2016;60:437–45.
22. Zhao S, Li L, Wang H, Zhang Y, Cheng X, Zhou N, et al. Wound dressings composed of copper-doped borate bioactive glass microfibers stimulate angiogenesis and heal full-thickness skin defects in a rodent model. Biomaterials. 2015;53:379–91.
23. Wray P. Cotton candy' that heals? Borate glass nanofibers look promising. Am Ceram Soc Bull. 2011;90(4):25–9.
24. Wray P. Wound healing: An update on Mo-Sci's novel borate glass fibers. Am Ceram Soc Bull. 2013;92(4):30–5.
25. http://etissuesolutions.com.in. 2020.
26. Serra R, Grande R, Butrico L, Rossi A, Settimio UF, Caroleo B, et al. Chronic wound infections: the role of *Pseudomonas aeruginosa* and *Staphylococcus aureus*. Expert Rev Anti Infect Ther. 2015;13(5):605–13.
27. Jung S, Day T, Boone T, Buziak B, Omar A "Anti-biofilm activity of two novel, borate based, bioactive glass wound dressings". Biomedical Glasses. 2019;5(1):67–75.
28. Rai M, Yadav A, Gade A. Silver nanoparticles as a new generation of antimicrobials. Biotechnol Adv. 2009;27(1):76–83.
29. Feng QL, Wu J, Chen GQ, Cui FZ, Kim TN, Kim JO. A mechanistic study of the antibacterial effect of silver ions on Escherichia coli and Staphylococcus aureus. J Biomed Mater Res. 2000;52(4):662–8.
30. Ahmed I, Abou Neel EA, Valappil SP, Nazhat SN, Pickup DM, Carta D, et al. The structure and properties of silver-doped phosphate-based glasses. J Mat. Sci. 2007;42(23):9827–35.
31. Nadworny PL, Wang JF, Tredget EE, Burrell RE. Anti-inflammatory activity of nanocrystalline silver in a porcine contact dermatitis model. Nanomedicine-Nanotechnology Biology and Medicine. 2008;4(3):241–51.
32. You C, Li Q, Wang X, Wu P, Ho JK, Jin R, et al. Silver nanoparticle loaded collagen/chitosan scaffolds promote wound healing via regulating fibroblast migration and macrophage activation. Sci. Rep. 2017;7[1].
33. Chernousova S, Epple M. Silver as antibacterial agent: ion, nanoparticle, and metal. Angew Chem Int Ed. 2013;52(6):1636–53.
34. Poon VKM, Burd A. In vitro cytotoxity of silver: implication for clinical wound care. Burns. 2004;30(2):140–7.
35. Naseri S, Lepry WC, Maisuria VB, Tufenkji N, Nazhat SN. Development and characterization of silver-doped sol-gel-derived borate glasses with anti-bacterial activity. J Non-Cryst Solids. 2019;505:438–46.
36. Wojtowicz AM, Oliveira S, Carlson MW, Zawadzka A, Rousseau CF, Baksh D. The importance of both fibroblasts and keratinocytes in a bilayered living cellular construct used in wound healing. Wound Repair Regen. 2014;22(2):246–55.
37. Park K, Amano H, Kashiwagi S, Shibuya M, Majima M, Takeda A. The role of vascular endothelial growth factor receptor 1 (Vegfr-1) signalling in wound healing. Wound Repair Regen. 2016;24(6):A4.
38. Bao P, Kodra A, Tomic-Canic M, Golinko MS, Ehrlich HP, Brem H. The role of vascular endothelial growth factor in wound healing. J Surg Res. 2009;153(2):347–58.
39. Barrientos S, Stojadinovic O, Golinko MS, Brem H, Tomic-Canic M. Growth factors and cytokines in wound healing. Wound Repair Regen. 2008;16(5):585–601.
40. Lu S, Xia D, Huang G, Jing H, Wang Y, Gu H. Concentration effect of gold nanoparticles on proliferation of keratinocytes. Colloids Surf, B. 2010;81(2):406–11.
41. Magyari K, Nagy-Simon T, Vulpoi A, Popescu RA, Licarete E, Stefan R, et al. Novel bioactive glass-AuNP composites for biomedical applications. Mater Sci Eng, C. 2017;76:752–9.
42. Neibert K, Gopishetty V, Grigoryev A, Tokarev I, Al-Hajaj N, Vorstenbosch J, et al. Wound-healing with mechanically robust and biodegradable hydrogel fibers loaded with silver nanoparticles. Adv Healthc Mater. 2012;1(5):621–30.
43. Chaloupka K, Malam Y, Seifalian AM. Nanosilver as a new generation of nanoproduct in biomedical applications. Trends Biotechnol. 2010;28(11):580–8.
44. Luo S-H, Xiao W, Wei X-J, Jia W-T, Zhang C-Q, Huang W-H, et al. In vitro evaluation of cytotoxicity of silver-containing borate bioactive glass. J Biomed Mater Res B. 2010;95B(2):441–8.

45. Cerruti M, Greenspan D, Powers K. Effect of pH and ionic strength on the reactivity of Bioglass 45S5. Biomaterials. 2005;26(14):1665–74.
46. Lepry WC, Naseri S, Nazhat SN. Effect of processing parameters on textural and bioactive properties of sol–gel-derived borate glasses. J Mat Sci. 2017;52(15):8973–85.
47. Lepry WC, Nazhat SN. Highly bioactive sol-gel-derived borate glasses. Chem Mater. 2015;27(13):4821–31.
48. Lepry WC, Rezabeigi E, Smith S, Nazhat SN. Dissolution and bioactivity of a sol-gel derived borate glass in six different solution media. Biomed Glasses. 2019;5(1):98–111.
49. Lepry WC, Smith S, Nazhat SN. Effect of sodium on bioactive sol-gel-derived borate glasses. J Non-Cryst Solids. 2018;500:141–8.
50. Lepry WC, Nazhat SN. The anomaly in bioactive sol–gel borate glasses. Mater Adv. 2020;1(5):1371–81.
51. Kaiser JP, Roesslein M, Diener L, Wichser A, Nowack B, Wick P. Cytotoxic effects of nanosilver are highly dependent on the chloride concentration and the presence of organic compounds in the cell culture media. J Nanobiotechnology. 2017;15.
52. Mikkelsen H, McMullan R, Filloux A. The pseudomonas aeruginosa reference strain PA14 displays increased virulence due to a mutation in ladS. PLoS One. 2011;6(12):e29113.
53. Stoor P, Soderling E, Salonen JI. Antibacterial effects of a bioactive glass paste on oral microorganisms. Acta Odontol Scand. 1998;56(3):161–5.
54. Stoor P, Söderling E, Grénman R. Bioactive glass S53P4 in repair of septal perforations and its interactions with the respiratory infection-associated microorganisms Heamophilus influenzae and Streptococcus pneumoniae. J Biomed Mater Res. 2001;58(1):113–20.
55. Yang Q, Chen S, Shi H, Xiao H, Ma Y. In vitro study of improved wound-healing effect of bioactive borate-based glass nano-/microfibers. Mater Sci Eng C Mater Biol Appl. 2015;55:105–17.
56. Brown RF, Rahaman MN, Dwilewicz AB, Huang W, Day DE, Li Y, et al. Effect of borate glass composition on its conversion to hydroxyapatite and on the proliferation of MC3T3-E1 cells. J Biomed Mater Res A. 2009;88A(2):392–400.
57. Frankova J, Pivodova V, Vagnerova H, Juranova J, Ulrichova J. Effects of silver nanoparticles on primary cell cultures of fibroblasts and keratinocytes in a wound-healing model. J Appl Biomater Funct Mater. 2016;14(2):e137–e142.
58. Liu X, Lee PY, Ho CM, Lui VC, Chen Y, Che CM, et al. Silver nanoparticles mediate differential responses in keratinocytes and fibroblasts during skin wound healing. ChemMedChem. 2010;5(3):468–75.
59. Burd A, Kwok CH, Hung SC, Chan HS, Gu H, Lam WK, et al. A comparative study of the cytotoxicity of silver-based dressings in monolayer cell, tissue explant, and animal models. Wound Repair Regen. 2007;15(1):94–104.
60. Morones-Ramirez JR, Winkler JA, Spina CS, Collins JJ. Silver enhances antibiotic activity against gram-negative bacteria. Sci Transl Med. 2013;5(190):190ra81.
61. Duan X, Peng D, Zhang Y, Huang Y, Liu X, Li R, et al. Subcytotoxic concentrations of ionic silver promote the proliferation of human keratinocytes by inducing the production of reactive oxygen species. Front Med. 2018;12(3):289–300.
62. Zhang K, Lui VC, Chen Y, Lok CN, Wong KK. Delayed application of silver nanoparticles reveals the role of early inflammation in burn wound healing. Sci. Rep. 2020;10(1):1–12.
63. Ottomeyer M, Mohammadkah A, Day D, Westenberg DJ. Broad-spectrum antibacterial characteristics of four novel borate-based bioactive glasses. Adv Microbiol. 2016;6(10):776–87.
64. Wang H, Zhao S, Cui X, Pan Y, Huang W, Ye S, et al. Evaluation of three-dimensional silver-doped borate bioactive glass scaffolds for bone repair: Biodegradability, biocompatibility, and antibacterial activity. J Mater Res. 2015;30(18):2722–35.

SUPPORTING INFORMATION

Additional supporting information may be found online in the Supporting Information section.

How to cite this article: Naseri S, Griffanti G, Lepry WC, Maisuria VB, Tufenkji N, Nazhat SN. Silver-doped sol-gel borate glasses: Dose-dependent effect on *Pseudomonas aeruginosa* biofilms and keratinocyte function. *J Am Ceram Soc*. 2021;00:1–12. https://doi.org/10.1111/jace.17802